

STUDY ON IMPACT LOAD RESPONSE OF THE PC SLEEPER FOR RAIL JOINT USING THREE-DIMENSIONAL NUMERICAL ANALYSIS MODEL

Shintaro Minoura^{1*}, Tsutomu Watanabe¹, Kodai Matsuoka¹, Hiroshi Yamane²

¹ Railway Technical Research Institute
2-8-38 Hikari-cho, Kokubunji-shi, Tokyo 185-8540 Japan
minoura.shintaro.51@rtri.or.jp, watanabe.tsutomu.30@rtri.or.jp, matsuoka.kodai.13@rtri.or.jp

² West Japan Railway Company
4-24, Shibata 2-chome, Kita-ku, Osaka 530-8341 Japan
hiroshi-yamane4@westjr.co.jp

Keywords: Prestressed Concrete Sleeper, Railway Track, Rail Joint, LS-DYNA, Impact Load, Dynamic Interaction

Abstract. *The purpose of this study is to clarify the influence of impact load due to train passing through the rail joint on the prestressed concrete sleeper (PC sleeper). The design of PC sleeper has been carried out in consideration of the influence of the impact load. Impact loads are caused by rail joints, irregularities of rail welded joints, rail corrugation, and wheel flat (damages generated on the wheel treads when the wheels slide on the rail running surface). Among them, the impact loads due to the rail joint and the wheel flats tend to be relatively large. In Japan, from the beginning of the development of the PC sleepers, the wheel flats have been recognized as one of the biggest factors of the impact load, and the studies on the influence of the impact load caused by the wheel flats on PC sleepers have been actively conducted. On the other hand, there have been few studies on the influence of the impact load caused by the rail joint on PC sleepers. In this study, we constructed a three-dimensional FE model of the PC sleeper which is able to simulate the nonlinear behavior of the PC sleeper. Using this analytical model, the influence of the impact load caused by the rail joint on the maximum bending moment and the stress generated in PC sleeper for various amounts of rail irregularity and various train speeds was quantitatively evaluated. In addition, the influence of parameters such as the amount of prestressing force, abrasion of PC sleeper, corrosion of PC steel wire were clarified. In the future, we plan to develop an optimum design method for PC sleeper for the rail joint considering the impact load caused by the rail joint using the result of the analysis.*

1 INTRODUCTION

The design of PC sleeper is carried out in consideration of the influence of the impact load. Impact loads are caused by rail joints, irregularities of rail welded joints, rail corrugation, and wheel flat (damages generated on the wheel treads when the wheels slide on the rail running surface). Among them, the impact loads due to the rail joint and the wheel flats tend to be relatively large. In Japan, from the beginning of the development of the PC sleepers, the wheel flats have been recognized as one of the biggest factors of the impact load and studies on the influence of the impact load caused by the wheel flats on PC sleepers have been actively conducted [1]. On the other hand, there have been few studies on the influence of the impact load caused by the rail joint on PC sleepers.

In the previous study, the numerical analysis with the beam model was executed, and the effect of the impact load due to the rail joint on PC sleeper was evaluated [2]. This previous study indicates that the supporting condition of the PC sleeper has the significant influence on the generated bending moment of the PC sleeper.

However, studies on the cracks generated in the PC sleeper due to the impact load, the effect of the wear of the bottom surface of the PC sleepers, the effect of the prestressing force and the effect of the corrosion of the PC steel wire are inadequate. To evaluate these effects with numerical analysis, it is necessary to construct a three-dimensional FE model considering nonlinearity of the material of the PC sleeper.

Based on the above background, we focused on the rail joint and constructed a nonlinear three-dimensional FE model reproducing the PC sleeper for the rail joint. Using this model, the influence of the various parameters on the bending moment and the stress of the PC sleeper for the rail joint were quantitatively evaluated.

2 ANALYSIS METHOD

2.1 Target PC sleeper

Figure 1 shows the target PC sleeper and rail joint section. The weight of the rail in this section is 60kg per meter and there are rail joints every 25m. The PC sleeper just under the rail joint is “PC sleeper for the rail joint” prescribed in Japanese Industrial Standards (JIS). Other sleepers are “type 6 PC sleeper” prescribed in JIS. Number of PC sleepers is 14 per 25m. The section is in a transition curve.

Figure 2 shows the attachment positions of the strain gauges, and Figure 3 shows the measurement method of the vibration mode of the PC sleeper. In order to compare the measurement results of the actual PC sleeper with the results of the numerical analysis, the bending moment and the vibration mode of the PC sleepers at the time of the train passing were measured. For the measurement of the bending moment, the strain gauges were attached to the

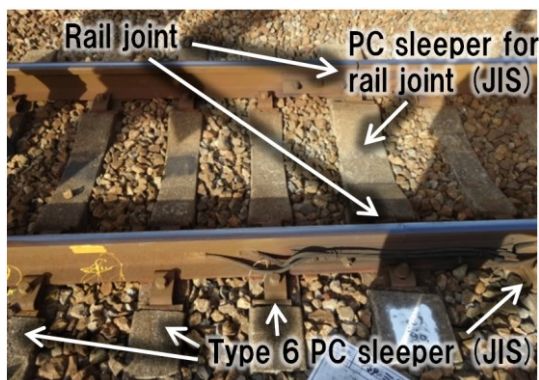


Figure 1: Target track structure

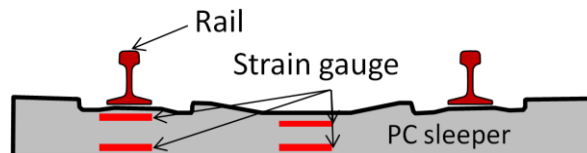


Figure 2: Attachment position of the strain gauge

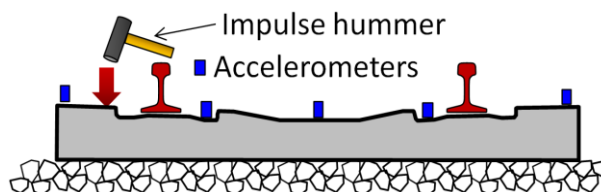


Figure 3: Measurement method of the vibration mode

cross section at the rail position and the center cross section, and the bending moment calculated from the measured strain. In the measurement of the vibration mode, five piezoelectric accelerometers (Rion PV-85) were placed at the positions shown in Figure 3, and the free vibration response by the impulse hammer was measured. The identification method of vibration mode is ERA (Eigensystem Realization Algorithm) method [3]. The running trains are the commuter vehicles for the 1067mm gauge line (wheel load of about 50kN).

2.2 Analysis model

Figure 4 shows the outline of the numerical analysis model and Figure 5 shows the analysis model of PC sleeper for the rail joint (JIS). In the analysis, three-dimensional nonlinear FEM analysis was performed using the structural analysis software LS-DYNA (Ver. R 8.0.0). For vehicles, car body, bogie and wheel axle are modeled as rigid. These rigid bodies are connected with springs and dampers. The rail is modeled with beam elements. Around the rail joint, there are 30 rail elements between the adjacent rail fastening devices. For other sections, there are 6 rail elements between the adjacent rail fastening devices. The PC sleeper for the rail joint is modeled as hexahedral solid element. PC steel wire and stirrup are modeled as beam elements. Concrete elements of the PC sleeper and PC steel wires and stirrups are modeled to be completely adhered to each other. The type 6 PC sleeper is modeled as a beam element. The prestressing force of the PC sleeper is reproduced by giving the initial stress in the axial direction to the PC steel wire. The number of elements in the FE model was 10792 elements, and the number of nodes is 13271 nodes.

Figure 6 shows rail surface irregularities at the rail joint section. In order to study the influence of the impact force generated due to the irregularities of the surface of the rail, irregularities of the rail surface around the rail joint were measured using a measuring machine having a length of 1m. The irregularities of the rail surface measured were input to the analysis model.

Table 1 shows the material properties used in the analysis. Properties of the respective materials are based on the design standards for Japanese railway structures and track components [4] [5]. From the vibration mode of the PC sleeper and the measurement results of the generated bending moment, the spring constant of the track pad was set to twice the nominal value

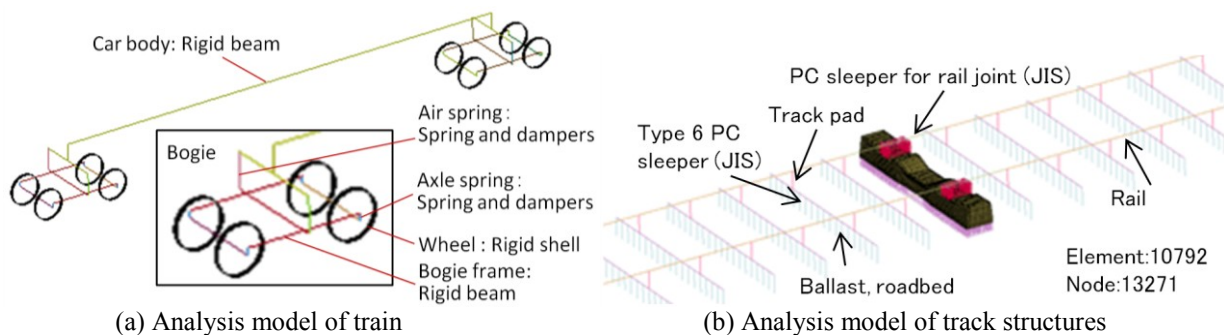


Figure 4: Outline of numerical analysis model

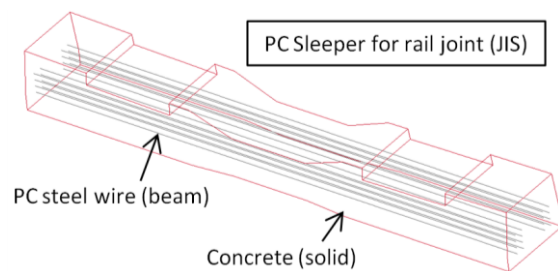


Figure 5: Analysis model of PC sleeper for rail joint

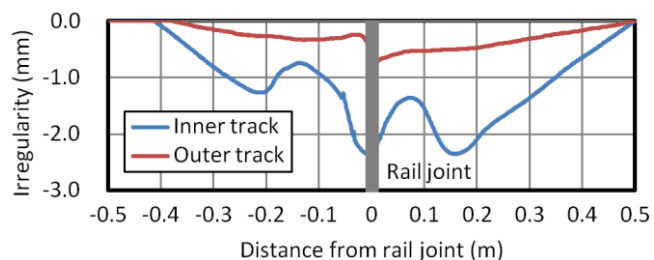


Figure 6: rail surface irregularities at the rail joint section

and the spring constant of the support of the PC sleeper was set to the value corresponding to the center supported state in which the spring constant of the support of PC sleeper at the center is larger than that of the support of PC sleeper at the rail position. Nearly a year has elapsed since the last implementation of maintenance work of the target PC sleeper and the rail joint section. So, it is considered that the compaction state of the ballast below the PC sleeper at the rail position loosened due to the impact of the train load and the support state of the PC sleeper shifted from the uniform support state to the center support state. In the section of 300mm in length around the center of the PC sleeper, twice the design value was used for spring constant of the support of the PC sleeper. The range of 300mm is a value estimated from the consistency between the actual measurement result and the analysis result concerning the vibration mode and the generated bending moment.

2.3 Analysis case

Table 2 shows the details of the analysis case. In this study, we evaluated the effect of the irregularity of the rail surface, prestressing force of the PC sleeper, wear of the bottom surface of the PC sleeper and corrosion of PC steel wires. The influence of the train speed on the irregularity of the rail surface was also evaluated. The irregularity of the rail surface is based on the measured value (the maximum amount of irregularity is 0.72mm for the outer rail,

Rail	Type: 60kg Rail (JIS) Young's modulus E_s : 200MPa
Track Pad	Spring Constant D_P : 220MN/m
Type 6 PC sleeper (JIS)	PC steel wire:dia.2.9mm*3 stranded wire, 12 Length L_P :2000mm, Bottom width B_P :240mm Height H_P :170mm(rail), 150mm(center) Young's modulus (concrete) E_C :49.5GPa
PC sleeper for rail joint (JIS)	PC steel wire:dia.2.9mm*3 stranded wire, 16 Length L_P :2000mm, Bottom width B_P :300mm Height H_P :170mm(rail), 145mm(center) Young's modulus (concrete) E_C :49.5GPa Tensile strength of concrete:3.08MPa
Ballast	Ballast thickness h :250mm Spring constant D_B :180MN/m(for 1 rail)
Roadbed	Ground reaction force coefficient K_{30} :110MN/m ³ Spring constant D_S :111MN/m(for 1 rail)

(In the range of 300 mm length near the center of the sleepers, spring constant of ballast spring and roadbed spring are doubled.)

Table 1: Material properties used in the analysis

Train speed V	30~130km/h (87km/h for basic case)
Rail surface irregularity δ	<ul style="list-style-type: none"> • <u>Measured value (maximum 0.72mm for outer rail, maximum 2.35mm for inner rail),</u> • Twice as measured value • Three times as measured value • Four times as measured value
Prestressing force	Ratio to the design value 100%, 50%, 30%, 20%, 10%, 0%
Wear of bottom surface	0mm, 10mm, 20mm
Corrosion of PC steel wire	<ul style="list-style-type: none"> • <u>No corrosion</u> • PC steel wire in the upper end of PC sleeper • PC steel wire in the lower end of PC sleeper

(Underlined value is for base case)

Table 2: Analysis case

2.35mm for the inner rail). In addition, the analysis was executed for the cases which the irregularity of the rail surface increased to double, three times and four times as large as the actual amount of the irregularity. As for the influence of the corrosion of the PC steel wires, the analysis was performed using the model without PC steel wire in the lower part of PC sleeper. It is assumed that the steel material corrodes due to cracks in the PC sleeper and becomes ineffective. As for the influence of the bottom wear, the analysis was carried out by deleting the solid element on the bottom surface and changing the size of the PC sleepers. The train running speed in the base case was set to 87km/h which is the speed at the time of the actual measurement.

3 ANALYSIS RESULTS

3.1 Vibration mode of the PC sleeper

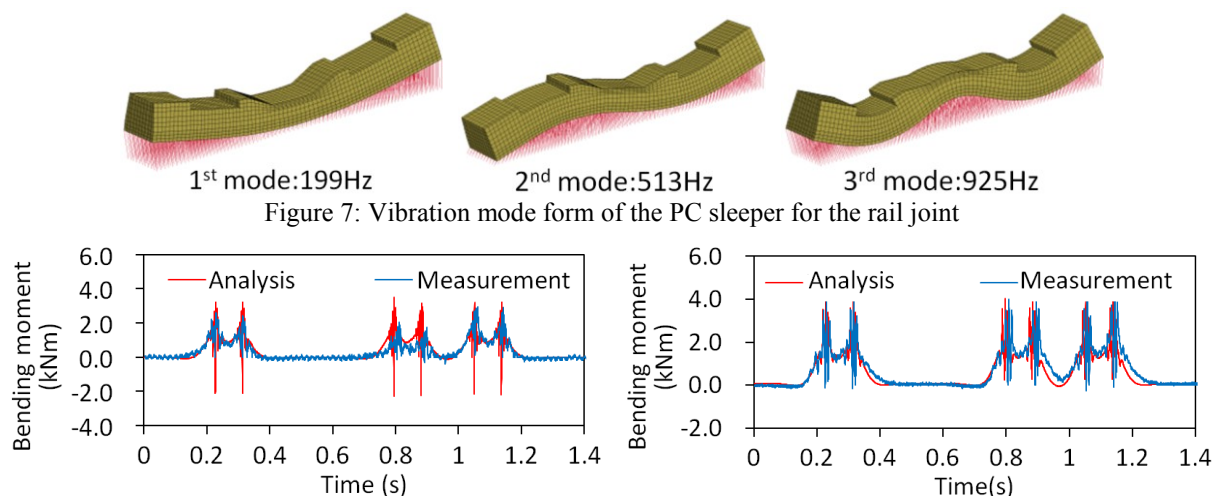
Table 3 shows the comparison between the actual measurement result and the analysis result of the vibration mode and the frequency of the PC sleeper for the rail joint. Figure 7 shows the vibration mode forms of the PC sleeper for the rail joint. For the PC sleeper for the rail joint, 101Hz as the translation mode in the vertical direction, 74Hz in the rotation mode, 202Hz in the first bending mode, 534 Hz in the second bending mode, and 907 Hz in the third bending mode were obtained. Comparing the natural frequencies of the actual measurement and the analysis, excluding the rotation mode, the differences between the natural frequencies of the measured value and the analysis results were within about 5%.

3.2 Bending moment of the PC sleeper

Figure 8 shows a comparison between the actual measurement results and the numerical analysis results with respect to the time history waveform of the bending moment of the PC sleeper for the rail joint when the train is passing. As shown in the figure, the maximum value of the negative bending moment at the center of the PC sleeper is larger than the positive bending moment at the rail position of the outer track side. From Figure 8 we can see that,

Vibration mode	Vertical translation	Rotation	1 st mode	2 nd mode	3 rd mode
Measured (Hz)	101	74	202	534	907
Analysis (Hz)	99	89	199	513	925

Table 3: Comparison between the measurement and the analysis of vibration mode of the PC sleeper for the rail joint



(a) Positive bending at rail position (outer rail)

(b) Negative bending at the center of the sleeper

Figure 8: Comparison between the measurement and the numerical analysis

although the negative moment instantaneously occurs at the rail position in the analysis, the analysis results and the actual measurement results generally agree with each other.

3.3 Effect of parameters

Figure 9 shows the effect of the irregularities of the rail surface on the maximum bending moment. The figure also shows the decompression moment and the crack generation moment used in the design for both the positive bending at the rail position and the negative bending at the center of the sleeper. From the figure, it is confirmed that the maximum moment increases as the irregularity becomes larger in all the cases. Moreover, the generated moment at the rail position of the inner rail side exceeds the crack generation moment to be considered in the design when irregularity of rail surface is 3 times or more as large as the actual measurement value. For the bending moment at the rail position cross section on the inner rail side, the generated moment in the case when the irregularities of the rail surface is four times as large as the actual value is smaller than that in the case where the irregularity is three times as large as the actual value. This is thought to be the influence of the train speed as described later.

Figure 10 shows the effect of each parameter on the maximum stress generated at the outermost edge of the PC sleepers. The stress value is positive for tension and negative for the compression. For the positive bending at the rail position cross section, the maximum stress at the bottom surface of the PC sleepers is shown in the figure, and for the negative bending at the center of the PC sleeper, the maximum stress at the top surface of the PC sleepers is shown in the figure. From the figure, it is confirmed that the crack generation stress is reached at the rail position cross section of the inner rail side in case where the irregularities of the rail

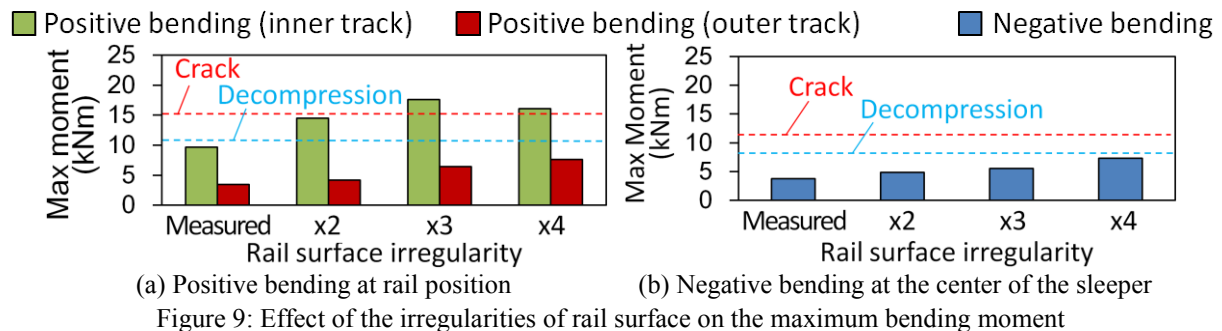


Figure 9: Effect of the irregularities of rail surface on the maximum bending moment

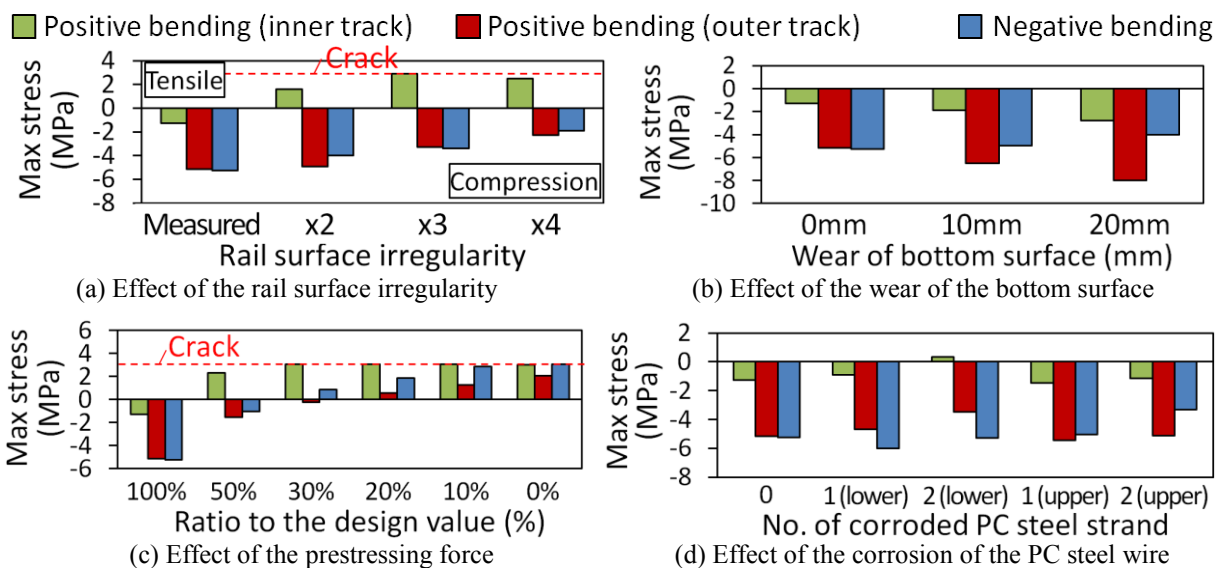


Figure 10: Effect of each parameter on the maximum stress

surface are tripled (the maximum irregularity on the inner rail side: 7.05mm).

For the bottom surface wear, it is confirmed that the maximum stress of negative bending increases due to the increase in amount of the wear. For the negative bending, the distance from the compressed edge of the PC sleeper to the PC steel wires is shortened with the increase of the wear of the bottom surface of the PC sleeper.

For the influence of prestressing force, if the prestressing force reduces to 30% of the initial prestressing force, cracks occur at the rail position on the inner race side, and cracks occur at the center of the PC sleeper if the prestressing force reduces to 10%.

For the influence of the corrosion of PC steel wires, the maximum stress in positive bending increases when the lowermost PC steel wire is removed, and the maximum stress of the positive bending at the rail position increases when the uppermost PC steel wire is removed.

Figure 11 shows the influence of the train running speed on the maximum bending moment for the various amounts of irregularity of the rail surface.

From the figure, the maximum bending moment tends to increase with the increase of irregularity of the rail surface and the train speed. However, for the maximum bending moment on the inner rail side, there is a peak observed at the running speed of around 70 km/h in the basic case, and there are peaks observed at the running speed around 30km/h, 70km/h, 120km/h in the case where the irregularity of the rail surface is 4 times as large as the actual measured value. It is confirmed from this fact that there is speed dependence with respect to the bending moment.

Although the profile of the measured irregularity of the rail surface of the inner rail is not a simple shape, it can be regarded that rail surface drops 2.35mm of the end of the length of rail of about 0.4m. Therefore, when the time at which the wheel takes to freely fall by 2.7 mm and the time at which the train takes to move by 0.4m along the rail coincide with each other, the amount of drop of the wheel becomes the maximum and the generated maximum moment is expected to increase. The train speed corresponding to the case is about 65km/h for the measured rail irregularity, about 46km/h for the case where the rail irregularity is twice as large as the measured value, and about 33km/h for the case where the rail irregularity is four times as large as the measured value. In each analysis case, since the peak appears at these speeds, the maximum moment of generated is considered to be influenced by the shape of the irregularity of the rail surface.

4 CONCLUSIONS

In this study, we constructed a nonlinear three-dimensional FE model reproducing the PC sleeper for the rail joint. Using this model, the influence of the various parameters on the bending moment and the stress of the PC sleeper for the rail joint were quantitatively evaluated.

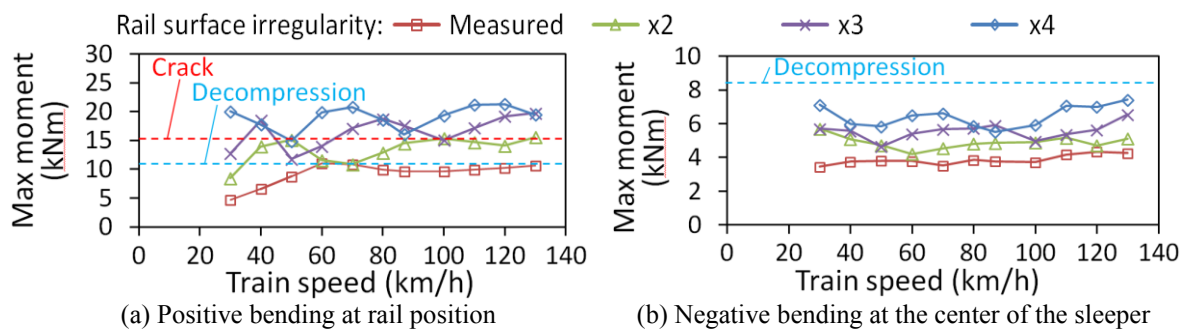


Figure 11: Influence of the train running speed on the maximum bending moment for the various amounts of irregularity of the rail surface

- According to the numerical analysis using the measured irregularity of the rail surface, the crack generates due to the train running at the speed of 87km/h when the irregularity of the rail surface is as three times as large as the measured value (the maximum amount of the irregularity on the inner rail side: 7.05mm)
- According to the analysis evaluating the effect of the corrosion of the PC steel wire, the generated maximum stress of the negative bending at the center of the sleeper increases in the case where the PC steel wire is removed assuming the bottom wear and corrosion of the steel wire at the upper end of the PC sleeper. In addition, the maximum stress of the positive bending at the rail position increases according to the analysis for the case where the PC steel wire at the bottom end of the PC sleeper is removed.
- According to the analysis, the cracks generated at the rail position of the inner track side in the case where the prestressing force is reduced to 30% of the initial prestressing force and the crack generated at the center of the PC sleeper in the case where prestressing force is reduced to 10% of the initial prestressing force.
- The bending moment of the PC sleeper has the characteristics of the speed dependency which is regarded as effect of the irregularity of the rail surface.

We will take these findings into the consideration in the design of the PC sleeper and to build an optimum design method of PC sleeper for the rail joint to cope with the impact load by the rail joint in the future research.

REFERENCES

- [1] H. Wakui, H. Okuda, A study on limit state design method for prestressed concrete sleepers, *Concrete library of JSCE*, No. 33, 1–25, June, 1999.
- [2] T. Watanabe, K. Matsuoka, S. Minoura, H. Yamane, Dynamic Response Characteristic of Prestressed Concrete Sleeper at Rail Joint, *Proceedings of the Japan Concrete Institute*, Vol.38, No.2, pp.985-990, 2016.(in Japanese)
- [3] K. Matsuoka, K. Kaito, H. Ishii, Statistical consideration regarding the vibration characteristics and variation factors of 24-span steel railway bridge in 86 years in service, *Journal of Japan Society of Civil Engineers F4*, Vol.68, No.3, pp.157-174, 2012. (in Japanese)
- [4] Railway Technical Research Institute, Design Standards for Railway Structures and Commentary (Track Structures), Maruzen Publishing Co. Ltd, 2004. (in Japanese)
- [5] Railway Technical Research Institute, Design Standards for Railway Structures and Commentary (Concrete Structures), Maruzen Publishing Co. Ltd, 2004. (in Japanese)